IEEE Photonics Journal
An IEEE Photonics Society Publication

Open Access

Continuously Operating Laser Range Finder Based on Incoherent Pulse Compression: Noise Analysis and Experiment

Volume 8, Number 2, April 2016

N. Arbel
L. Hirschbrand
S. Weiss
N. Levanon
A. Zadok

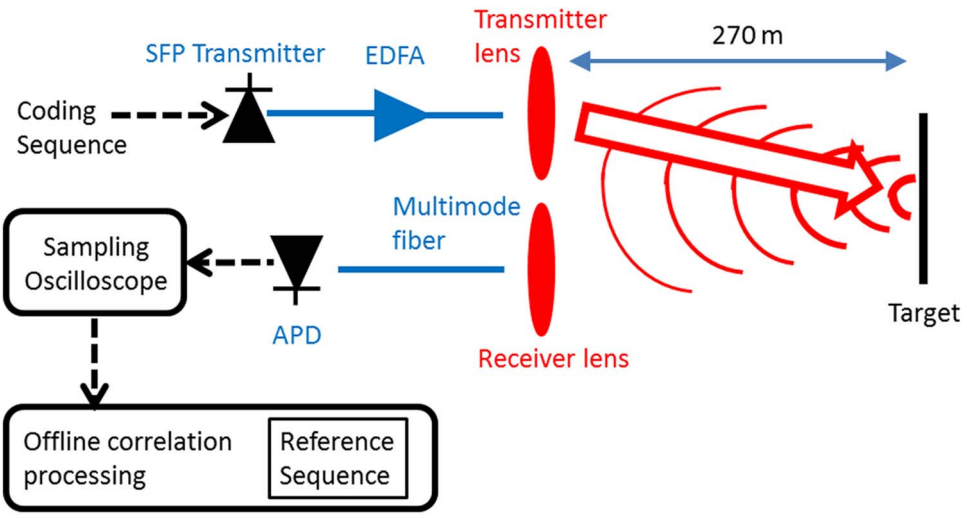

DOI: 10.1109/JPHOT.2016.2528118
1943-0655

Continuously Operating Laser Range Finder Based on Incoherent Pulse Compression: Noise Analysis and Experiment

N. Arbel,[1] L. Hirschbrand,[1] S. Weiss,[1] N. Levanon,[2] and A. Zadok[1]

[1]Faculty of Engineering, Bar-Ilan University, Ramat Gan 5290002, Israel
[2]Faculty of Engineering, Tel Aviv University, Tel Aviv 6997801, Israel

DOI: 10.1109/JPHOT.2016.2528118

Manuscript received November 24, 2015; revised February 4, 2016; accepted February 7, 2016. Date of publication February 11, 2016; date of current version February 22, 2016. Corresponding author: A. Zadok (e-mail: Avinoam.Zadok@biu.ac.il).

Abstract: A continuously operating laser range-finder setup based on the incoherent compression of periodic binary unipolar sequences is analyzed and demonstrated experimentally. The periodic cross-correlation between the directly detected echoes and a properly chosen reference sequence exhibits perfect zero sidelobes. An approximate analytic model for the peak-to-noise-sidelobe ratio in the presence of additive detector noise is established. Tradeoffs among transmitted power, measurement range, aperture size, and acquisition time are addressed. Performance is compared against that of time-of-flight measurements, and scenarios in which each protocol is advantageous are discussed. Outdoor ranging measurements at a distance of 270-m and with a ranging resolution of 15 cm are reported. The range to a Lambertian reflector target at that distance could be measured using a peak transmission power of only 800 mW, at a low signal-to-noise ratio (SNR) of −25 dB and with an acquisition time of 50 μs.

Index Terms: Lidar, fiber optics links and subsystems, laser range-finder.

1. Introduction

Laser range finders are widely employed in many civilian and military applications [1], [2]. They provide the basis for light detection and ranging (lidar) systems and for 3-D imaging cameras [3]. The most widely employed laser ranging protocol relies on the transmission of short and intense isolated pulses, and the measurement of the two-way time-of-flight (ToF) of echoes reflected from a target [1], [2]. ToF measurements are conceptually simple and provide good signal to noise ratios (SNRs). On the other hand, the instantaneous peak power of transmitted pulses in km-range ToF range-finders reaches kW levels, rendering them more vulnerable to interception by an adversary. In addition, ToF transmitters typically rely on Q-switched or mode-locked laser sources, which are often comparatively bulky and expensive.

Alternatively, the range to a target may be obtained based on the transmission of sequences of pulses and the compression of collected echoes by a proper post-detection procedure. Sequence coding is widely employed in radio-frequency (RF) and microwave radar systems [4], [5]. The entire energy of the long, coded waveform is effectively compressed post-detection,

into a narrow virtual peak. The SNR of the processed trace scales with the duration of the entire sequence, whereas the ranging resolution is governed by the duration of a single symbol within the code [4], [5]. The instantaneous power of the transmitted waveforms is orders of magnitude lower than that of ToF range finders. Moreover, the range-finder transmitter can be realized using simple direct modulation of low-cost, semiconductor laser diodes, followed by standard fiber or semiconductor optical amplifiers. Analog noise may also be used in laser range-finders. An implementation based on the broadband amplified spontaneous emission of an erbium-doped fiber amplifier (EDFA), or on the modulation of an optical carrier by broadband RF noise, was reported in [6].

Effective sequence compression with low residual sidelobes typically requires the transmission and coherent detection of phase information. On the other hand, direct detection of magnitude only is much simpler to implement in optical systems. In 2006, Levanon had proposed a protocol for the incoherent compression of unipolar binary sequences [7], and a first demonstration of the method in a laser range-finder experiment was reported by our group in 2012 [8]. Other optical applications of incoherent sequence compression in optics include distributed fiber sensors [9], and image resolution enhancement [10].

Initially the incoherent compression protocol could only support aperiodic sequences, separated by dead-time intervals [7], [8]. Recently, the mathematical formalism was extended to the incoherent compression of periodic sequences, allowing for the coding of continuous transmission without breaks [11], [12]. The formalism was addressed at length in a signal processing-oriented paper [11], where a laser range-finder experiment was discussed only briefly [11]. The current report is dedicated to the analysis and demonstration of the incoherent compression of periodic sequences in a continuously-operating laser range-finder, from an optics perspective.

The specific codes used are introduced in Section 2. In ideal, noise-free conditions, the compression of the chosen codes provides range sidelobes of exactly zero. Section 3 is dedicated to the performance analysis of incoherent sequence compression in the presence of additive detector noise, which is the dominant noise mechanism in practical setups. Additive noise leads to the formation of finite sidelobes. An approximate, analytic model for the peak-to-noise-sidelobe ratio (PNSLR) is provided and validated by numerical simulations. Performance bounds and tradeoffs among range, acquisition time, transmitted power and aperture diameter, imposed by additive noise, are addressed. Next, the comparison between ToF measurement protocols and incoherent compression is discussed in Section 4. We show that the former is superior in applications that are restricted by energy consumption, whereas the latter is advantageous when the probability of intercept and/or hardware simplicity is the primary consideration.

Last, ranging experiments up to a distance of 270 m, with a resolution of 15 cm, are reported in Section 5. The experiments validate the proposed relation between system PNSLR and SNR. Compared with our initial demonstration [8], the measurement range is increased more than five-fold. The peak transmission power was as low as 800 mW, and the range to a target could be identified at SNR levels as low as –25 dB with an acquisition time of 50 μs. Two targets at different depths, both in partial overlap with the range-finder beam, could be properly separated. The results demonstrate the applicability of the incoherent compression protocol for laser range-finder and lidar applications. A summary is given in Section 6.

2. Incoherent Compression of Periodic Sequences

Legendre sequences L_m,$m = 1, \ldots, N$ are binary phase codes, available at lengths $N = 4\kappa - 1$ where κ is an integer and N a prime [11], [13]. There are 519 available Legendre sequence lengths between $N = 1000$ and $N = 10\,000$. The code used in this work is 4003 bits-long. An element L_m in the code equals 1 if m is a quadratic residue modulo N: if an integer l exists such that l^2 mod $N = m$ mod N. If m is not a quadratic residue modulo N, then $L_m = -1$ instead. The periodic auto-correlation of L_m has a peak value of N at offsets that are integer multiples of N, and all its sidelobes are equal to –1.

Incoherent compression relies on the periodic transmission and direct detection of a unipolar version of the Legendre sequence, $\hat{L_m}$, in which every "–1" symbol in the original L_m is replaced by "0." The collected echo of $\hat{L_m}$ is cross-correlated with the original bipolar sequence L_m, which is digitally stored at the laser range-finder receiver as a reference:

$$c_n = \sum_{k=0}^{N-1} \hat{L}_k L_{(k+n) \bmod N}. \tag{1}$$

The transmission or detection of phase information is not required. The periodic cross-correlation between the two sequences is *perfect*: c_n assumes peak values for offsets that are integer multiples of N, and sidelobe values of exactly zero for all other offsets. The magnitude of the correlation peaks equals the number of "1" symbols in the sequence: $1/2(N+1)$. An example of an 11 elements Legendre bipolar reference sequence is: $L = [1, -1, 1, -1, -1, -1, 1, 1, 1, -1, 1]$. The corresponding unipolar transmitted sequence is: $\hat{L} = [1, 0, 1, 0, 0, 0, 1, 1, 1, 0, 1]$. It should be pointed out that perfect periodic cross-correlation between a bipolar m-sequence and its unipolar version was reported in [14]. In practical laser range-finder implementations, however, nonzero sidelobes are generated due to additive detector noise, as discussed next.

3. Incoherent Compression in the Presence of Additive Noise

Consider a laser range-finder in which the duration of each symbol in the transmitted code $\hat{L_m}$ is τ, and the average transmitted power is P_t. The optical power of transmitted "1" symbol pulses is therefore about $2P_t$, while no power is transmitted during "0" symbols. The ranging resolution provided is $\Delta z = 1/2c\tau$, and the range of unambiguous measurements is $N \cdot \Delta z$ (For possible solutions to range ambiguity see [15]). We assume that the transmitted beam is reflected from a target whose surface area is larger than that of the incident beam, located at a distance R. A fraction ρ of the incident optical power is reflected from the target surface. We suppose further that the angular distribution of the reflected optical wavefront follows a Lambertian profile. Subject to these conditions, the average optical power that is collected by a receiver with an optical aperture of diameter D is given by

$$P_r = \frac{D^2}{4R^2} \rho P_t. \tag{2}$$

The voltage at the output of the receiver photo-detector and its amplification circuitry is sampled at τ intervals to generate a sequence S_m which is a scaled replica of $\hat{L_m}$: $S_m = 2R_D P_t \hat{L_m}$, where R_D is the responsivity of the receiver in [V/W]. Since our setup includes only short fiber paths, we do not encounter pulse broadening in our measurements. The detected sequence is subject to additive noise n_m, due to thermal current fluctuations in the electronic circuitry. The received power P_r in our experiments is typically weak, on the order of 1–10 nW. In these conditions, detector noise is 2–3 orders of magnitude stronger than the intended signal. On the other hand, optical noise sources, such as laser intensity noise or the beating of signal with amplifier spontaneous emission, are much weaker than the intended signal. The process n_m is well-modeled as a white, zero-mean Gaussian noise, and it is often quantified in terms of the noise-equivalent power (*NEP*, in units of $W/\sqrt{Hz}$): the incident optical power that is required to achieve an SNR of unity, when measured at an electrical bandwidth of 1 Hz. The variance of n_m is given by: $\sigma_n^2 = R_D^2 NEP^2 \Delta f$, where Δf is the integration bandwidth of the photo-receiver. The measurement SNR is defined as the ratio between the average photo-current squared and the variance of the noise photo-current

$$SNR = \frac{R_D^2 P_r^2}{R_D^2 \cdot NEP^2 \cdot \Delta f} \approx \frac{\rho^2 D^4}{16R^4} \frac{P_t^2 \tau}{NEP^2}. \tag{3}$$

In (3), it is assumed that Δf is matched with the symbol duration: $\Delta f \approx 1/\tau$.

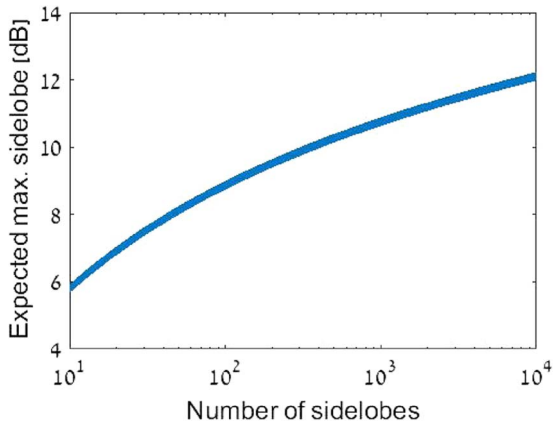

Fig. 1. Calculated expectation values of the magnitude of the highest sidelobe (in dB) as a function of the number of sidelobes considered. The maximum magnitudes are normalized to the average sidelobe magnitude.

The detected sequence $S_m + n_m$ is truncated to a length of M symbols and correlated with the reference sequence L_m. For simplicity we assume that M is an integer multiple of the Legendre code length N. The periodic cross-correlation values are of Gaussian statistics. Their expectation values are $C_0 = [M(N+1)/N] \cdot R_D P_r \approx M R_D P_r$ for offsets that are integer multiples of N, and zero for all sidelobes. The contribution of the signal S_m to the sidelobes of the cross-correlation is identically zero because of the perfect cross-correlation between $\hat{L_m}$ and L_m, and the contribution of the noise is of zero mean. The variance of the correlation outcome, for all offsets, is $\sigma_c^2 = M \cdot \sigma_n^2$. We may define the SNR following the cross-correlation operation as the ratio between the magnitude squared of the correlation peak C_0 and the noise variance:

$$\mathrm{SNR}_{\mathrm{corr}} \equiv \frac{C_0^2}{\sigma_c^2} \approx M \cdot \mathrm{SNR} = \frac{\rho^2 D^4}{16 R^4} \frac{P_t^2 T}{\mathrm{NEP}^2}. \tag{4}$$

Here, $T = M\tau$ is the acquisition duration.

Let us denote the magnitude squared of an individual correlation sidelobe as x. The probability distribution function (PDF) of x is a chi-squared distribution with a single degree of freedom, mean value $\langle x \rangle = \sigma_c^2$ and variance $\sigma_x^2 = 2\langle x \rangle^2$. The explicit form of the PDF is [16]

$$P\left(y \equiv \frac{x}{\langle x \rangle}\right) = \begin{cases} \frac{1}{\sqrt{2\pi y}} \exp\left(\frac{-y}{2}\right) = \frac{1}{\sqrt{\frac{2\pi x}{\langle x \rangle}}} \exp\left(\frac{-x}{2\langle x \rangle}\right), & y > 0 \\ 0, & \text{else} \end{cases} \tag{5}$$

where $y = x/\langle x \rangle$ The cumulative distribution function (CDF) of y is given by $F(y) = \int_0^y p(y')dy' = (1/\sqrt{\pi}) \cdot \gamma(1/2, y/2)$, where γ denotes the lower incomplete gamma function.

The PDF of the highest magnitude sidelobe $\max(y)$, among N_{sl} sidelobes within the measurement range of interest, may be approximated based on order statistics

$$P_{\max(y),N_{sl}}(y) = N_{sl}[F(y)]^{N_{sl}-1} p(y). \tag{6}$$

The expectation value of the highest normalized sidelobe, denoted as $\langle \max(y) \rangle$, may be calculated for each choice of N_{sl} based on (6): $\langle \max(y) \rangle = \int_0^\infty y P_{\max(y),N_{sl}}(y)dy$. The calculated results are shown in Fig. 1. In our experiments (reported in Section 5) we consider $N_{sl} = 200$ sidelobes. For that choice $\langle \max(y) \rangle = 9.5$ dB. Note that (6) is strictly valid only when the sidelobes are statistically independent, a condition that is not met by the processed traces (see the Appendix). Nevertheless, it still provides useful estimates for PNSLR statistics, as discussed later in this section.

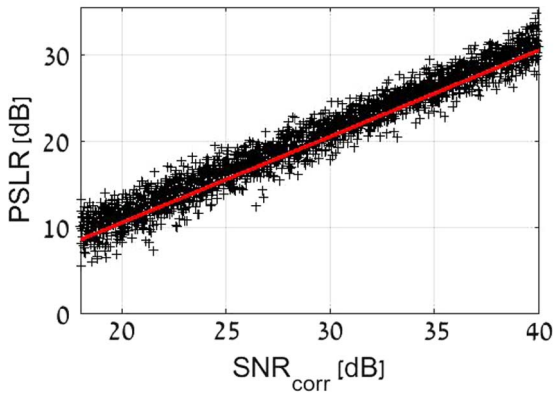

Fig. 2. Plus signs: simulated peak-to-noise-sidelobe ratios (PNSLRs) of 3000 realizations of a 4003 bits-long Legendre sequence, with additive noise at different signal-to-noise ratios (SNRs), following incoherent compression. Results are plotted against the SNR following correlation. Two hundred sidelobes were considered in each realization. Solid line: estimate for the expectation values of the PNSLRs, based on the approximation that the maximum among 200 sidelobes is 9.5 dB higher than the average one (see the approximate probability distribution function of the highest sidelobes magnitude, given in (6), and the relation to measurement SNR in (7)). The line is not a fit to the simulations results.

Using these results, the expected PNSLR of the processed trace may be estimated based to the measurement SNR

$$\langle \text{PNSLR} \rangle \equiv \frac{C_0^2}{\langle \max(x) \rangle} = \frac{C_0^2}{\langle \max(y) \rangle \langle x \rangle} = \frac{C_0^2}{\langle \max(y) \rangle \sigma_c^2} = \frac{\text{SNR}_{\text{corr}}}{\langle \max(y) \rangle} = \frac{M \cdot \text{SNR}}{\langle \max(y) \rangle}. \tag{7}$$

We therefore expect a PNSLR that is 9.5 dB lower than SNR_{corr} in our experiments.

The validity of (7) was tested through numerical simulations of the incoherent compression of $\hat{L_m}$, in the presence of additive noise with different values of σ_n^2. The length of the simulated traces M was chosen to match the code period N. Fig. 2 shows a scatter diagram of the calculated PNSLR values as a function of SNR_{corr}, for 3000 realizations (plus signs). The straight solid line denotes $\langle \text{PNSLR} \rangle$ based on (7). A linear fit to the numerical results yields a slope of 1.01 and an intercept of –8.7 dB. The root-mean-squared difference between the predicted and calculated PNSLR levels is 1.5 dB.

General agreement between model and simulations is good. However, the numerically obtained intercept of the fitted PNSLR curve is 0.8 dB higher than the –9.5 dB value predicted in Fig. 1. The difference is due to residual statistical dependence among the sidelobes. Fig. 3 shows the numerically obtained histogram of $\max(y)$ for $N_{sl} = 200$ sidelobes, alongside the PDF of (6). Their comparison reveals that the model overestimates $\langle \text{PNSLR} \rangle$ by approximately 0.8 dB. This difference is insignificant from a system standpoint, since it is smaller than the scatter in the simulated PNSLR values. The overestimate of the model becomes even smaller when the number of sidelobes considered is increased (0.5 dB for $N_{sl} = N - 1 = 4,002$, representing the longest range of unambiguous measurements).

In order to reduce the probability of false acquisitions, we arbitrarily define the minimum acceptable PNSLR: $\text{PNSLR}_{\text{min}} = 10$. Based on this criterion and Eq (7), we may estimate the minimum required value of SNR_{corr}, $\text{SNR}_{\text{corr}}^{\text{min}} \equiv \text{PNSLR}_{\text{min}} \langle \max(y) \rangle$. Noise sidelobes considerations set trade offs among range, aperture size, transmission power, and acquisition duration:

$$\text{SNR}_{\text{corr}} = \frac{\rho^2 D^4}{16 R^4} \frac{P_t^2 T}{\text{NEP}^2} \geq \text{SNR}_{\text{corr}}^{\text{min}} \approx 100. \tag{8}$$

This expression serves as a useful guideline for system design.

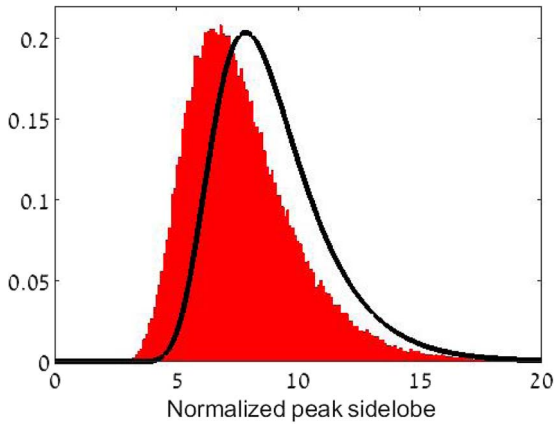

Fig. 3. Histogram of highest sidelobe magnitude values of a 4003 bits-long Legendre sequence with additive noise, following incoherent compression (red). The peak sidelobe magnitudes are normalized to the average sidelobe magnitude. The histogram was calculated based on 100000 additive noise realizations. The highest among 200 sidelobes was considered in each. The black curve shows the approximate probability distribution function of the highest sidelobe; see (6).

4. Comparison Between Sequence Compression and Time-of-Flight Laser Range Finders

It is worthwhile to compare the performance of a laser range-finder based on incoherent pulse compression with that of a ToF implementation. The two systems are, in principle, equivalent under noise-free conditions. However, performance could become markedly different when additive noise is considered. We suppose that both systems use the same receiver and the same collection aperture, and provide the same resolution Δz and measurement repetition rate $1/T$. The performance of a ToF laser range finder is evaluated based on the SNR of a single sample of the detector output, whereas that of the sequence coded implementation is evaluated based on the output of the correlation operation.

A comparison can be drawn based on two possible constraints, depending on application. In a so-called "energy-limited" range-finder, it is assumed that the two systems transmit equal overall energy E per acquisition. P_t of the sequence-coded range finder would then be E/T, leading to

$$\mathrm{SNR}_{\mathrm{corr}} \approx \frac{\rho^2 D^4}{16R^4}\frac{1}{\mathrm{NEP}^2}\frac{E^2}{T}. \tag{9}$$

In contrast, the transmitted power of a single pulse in a ToF range finder would be $P_{\mathrm{peak}} = E/\tau$, with a measurement SNR of

$$\mathrm{SNR}_{\mathrm{ToF}} \approx \frac{\rho^2 D^4}{16R^4}\frac{1}{\mathrm{NEP}^2}\frac{E^2}{\tau} = M \cdot \mathrm{SNR}_{\mathrm{corr}}. \tag{10}$$

For equal energy consumption, resolution, repetition rate and aperture size, and using the same detector, the SNR provided by a time-of-flight laser range-finder would be orders of magnitude higher than that obtained using incoherent compression. On the other hand, in so-called "power-limited" applications, the constraint on transmission is the maximum available peak power, rather than the overall energy. If P_{peak} of a ToF system is restricted to $2P_t$ of a corresponding sequence-coded realization, we find that

$$\mathrm{SNR}_{\mathrm{ToF}} \approx \frac{\rho^2 D^4}{16R^4}\frac{4P_t^2\tau}{\mathrm{NEP}^2} = \frac{4}{M}\mathrm{SNR}_{\mathrm{corr}}. \tag{11}$$

The preference of one implementation over the other is therefore critically dependent on the circumstances of the specific application at hand. The above comparison does not take into account potential complexity or cost associated with the generation of short and intense pulses.

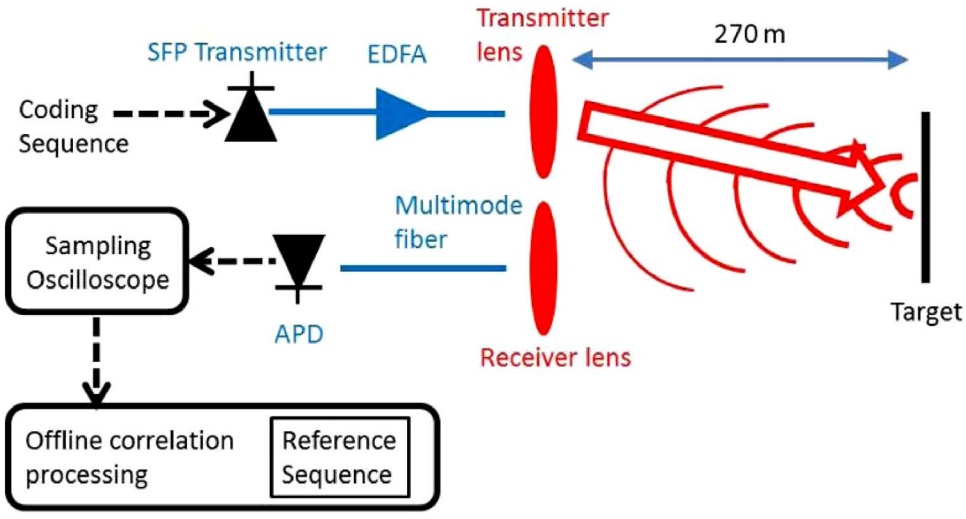

Fig. 4. Experimental setup for a laser range-finder based on the incoherent compression of periodic sequences. SFP: small form-factor pluggable. EDFA: erbium-doped fiber amplifier. APD: avalanche photo-diode. Solid blue lines denote fiber-optic paths. Dashed black lines denote radio-frequency cable paths. Red denotes free-space propagation.

5. Outdoor Ranging Experiments

Fig. 4 shows the experimental setup used in laser range-finder experiments based on the incoherent pulse compression of repeating, periodic sequences. A small form-factor pluggable (SFP) gigabit Ethernet transmitter module at 1550 nm wavelength was used to generate the optical waveform. The output power of the laser diode in the SFP module was directly modulated by the output voltage of an arbitrary waveform generator (AWG), programmed to repeatedly generate the unipolar representation of a Legendre sequence $\hat{L_m}$ of length $N = 4003$ bits. The duration τ of each symbol within the code was 1 ns, corresponding to an anticipated ranging resolution Δz of 15 cm. The average optical power at the output of the SFP transmitter was −3 dBm. The modulated waveform was amplified to an average power P_t of 400 mW by an EDFA, expanded by a collimating lens of 9 cm diameter and launched towards potential targets.

A regular, white sheet of paper was placed at various distances from the laser range-finder setup. The power reflectivity of the paper surface ρ was measured in a separate experiment to be 0.07. The optical waveform reflected from the target was partially collected by a second lens of $D = 9$ cm diameter into a multimode fiber of 200 μm core diameter. The far end of the fiber was connected to an InGaAs avalanche photo-diode (APD) of 1 GHz bandwidth and *NEP* of 0.6 $pW/\sqrt{Hz}$. The APD and its associated amplification circuitry provided a responsivity of 40 kV/W. The standard deviation of noise at the output of the receiver was 800 μV. The signal at the output of the APD was sampled by a real-time digitizing oscilloscope of 6 GHz bandwidth. The sampling circuitry contributed a second source of additive Gaussian noise with a standard deviation of 300 μV. The overall σ_n of the measurement setup was therefore 850 μV. The sampled waveform was correlated with the reference sequence L_m using off-line processing.

Initial, coarse alignment between the transmission and receiving apertures was performed using two visible light sources. The output of one source was launched towards the target through the transmission lens, temporarily replacing the EDFA output, and the output of another was connected in place of the APD and directed towards the target through the multimode fiber and the receiving aperture. The positions of the fibers leading into the lenses were carefully adjusted using three-axis linear stages until the two visible light spots were in overlap on the target surface.

Next, the output of the EDFA was reconnected to the transmission aperture, and the average collected optical power P_r at the output of the multimode fiber was measured by

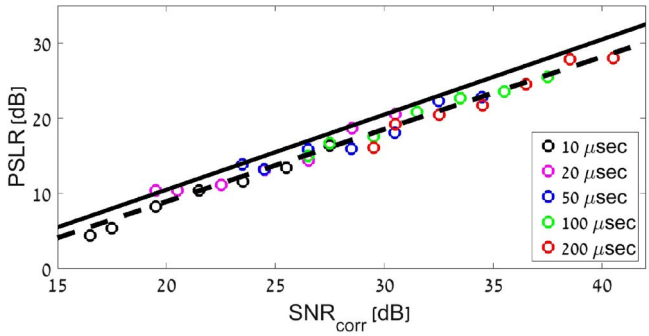

Fig. 5. Circles: measured peak-to-noise-side-lobe ratios (PNSLRs) of repeating, 4003 bits-long Legendre sequences, collected in reflection from a target at 100 m distance in indoors laser range-finder experiments. PNSLRs were noted following the incoherent compression of the collected echoes. Experiments were carried out using different acquisition times between 10–200 μs (see legend for colors) and at different SNR levels. Solid line: predicted PNSLR values. Dashed line: linear regression of experimental PNSLR values. The mean offset between predicted and observed PNSLR values is only 0.8 dB.

a low-bandwidth optical power meter. The axial positions of both fibers were fine-tuned to optimize focus and maximize P_r. Following these alignment procedures, the APD was reconnected to the multimode fiber output, and reflected sequence echoes were detected to perform ranging measurements.

In a first experiment, measurements were taken for an indoors target at 100 m distance, at different SNR levels and acquisition durations T. PNSLRs were noted as the relative magnitude of the highest among 200 sidelobes considered in each measurement. Fig. 5 shows the obtained PNSLR levels as a function of $\mathrm{SNR_{corr}}$ (circle symbols). Colors denote the acquisition durations (see legend). Data collected with different acquisition durations fit on a single curve. A linear fit to the measured PNSLRs (dashed line) yields a slope of 0.963 and an intercept of −10.3 dB. Agreement between model and experiment is therefore very good. The difference between predicted and measured PNSLRs is only 0.8 dB (see Figs. 1 and 2). The results demonstrate that the experimental performance of the laser range-finder is limited by additive detector noise.

In a second experiment, the target was placed outdoors at 270 m distance. The diameter of the transmitted beam on the target surface was 20 cm. The average collected optical power was −59 dBm, in good agreement with (2). The measurements were carried out at night. The power of background light coupled into the receiver was below the noise floor of our low-bandwidth power meter (−70 dBm). The measurement SNR was −25 dB. Fig. 6 shows the compressed form of a reflected echo, acquired over about 48 μs ($M = 48\,036$, $\mathrm{SNR_{corr}}$ of 22 dB). The full-width at half maximum of the main correlation peak was 14 cm, and the PNSLR of the compressed trace was 14 dB, within 1 dB of prediction. Fig. 7 shows the measured PNSLRs for several experiments as a function of $\mathrm{SNR_{corr}}$. While deviations from predicted values are somewhat larger than those of Fig. 5, the agreement remains good.

In a third set of experiments, the transmitted beam was aligned to be in partial overlap with two white paper targets, separated in depth by 1.2 m, at a distance of 273 m. The incoherently compressed form of the reflected echo is shown in Fig. 8. The analysis of the trace could recover the two targets with the expected separation.

6. Summary

A continuously-operating laser range-finder setup, based on a recently-proposed protocol for the incoherent compression of periodic unipolar sequences, was analyzed and demonstrated experimentally. The measurement is based on simple direct detection, and the transmission or acquisition of phase information is not required. The periodic cross-correlation between the transmitted unipolar sequence and its reference is mathematically perfect, with zero off-peak sidelobes.

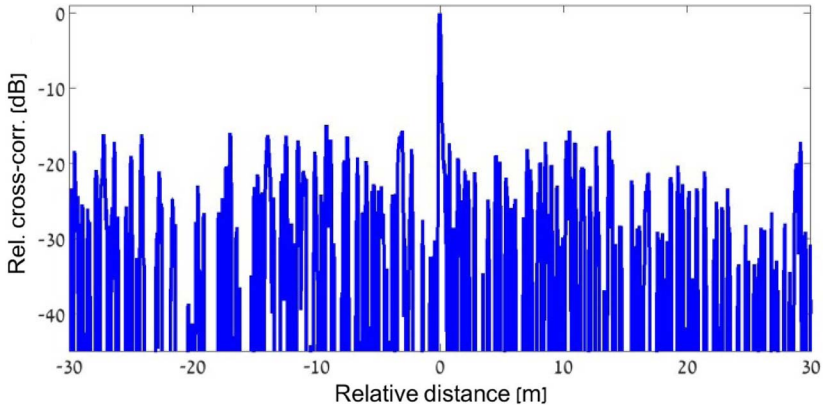

Fig. 6. Incoherently compressed form of a continuously operating laser range-finder trace, following reflection from an outdoor target at a distance of 270 m. The intensity of the transmitted waveform was repeatedly modulated by a unipolar representation of a 4003 bits-long Legendre sequence, with a symbol duration of 1 ns (ranging resolution of 15 cm). The trace was acquired at an SNR of −25 dB over 48 μs.

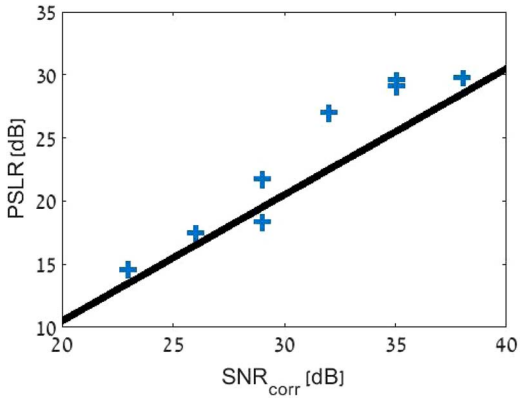

Fig. 7. Plus signs: measured peak-to-noise-sidelobe ratios (PNSLRs) of repeating, 4003 bits-long Legendre sequences, collected in reflection from a target at a distance of 270 m in outdoor laser range-finder experiments. PNSLRs were noted following the incoherent compression of the collected echoes. Solid line: predicted PNSLR values.

The results extend upon our previous reports in several respects: An approximate analytic model for sidelobe magnitude statistics in the presence of detector noise is provided. The model is supported by numerical simulations and controlled indoor experiments. Tradeoffs among range, aperture size, transmission power, and acquisition duration are identified. These tradeoffs serve as guidelines for system design. A comparison between the performance of an incoherently compressed range-finder and of one that is based on ToF is given, and potential applications in which each embodiment would be advantageous are discussed. While a ToF configuration would provide better performance for systems that are restricted by their energy consumption, incoherent compression is favorable when peak power is the most significant consideration.

The demonstration of the incoherent compression-based range finder is extended to outdoor experiments at 270 m range. The measurement distance is more than five times longer than that of the previous demonstration. The range to the target could be measured at SNR conditions as low as −25 dB, with peak transmitted power levels of 800 mW only, and with acquisition times of only 50 μs. The ability to distinguish between two targets at closely spaced depths is demonstrated as well.

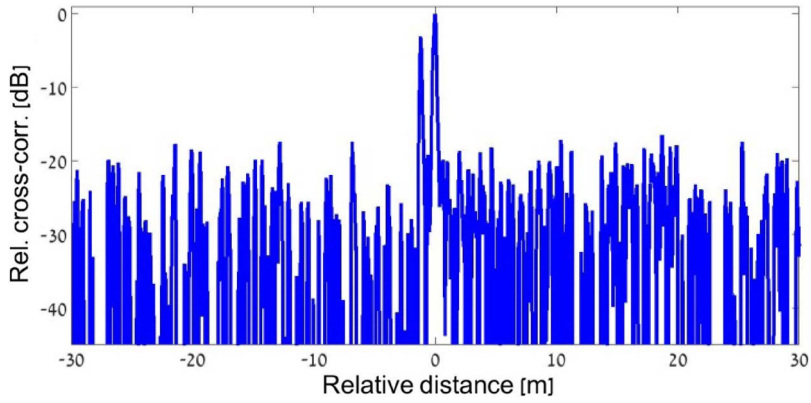

Fig. 8. Incoherently compressed form of a continuously operating laser range-finder trace, following reflection from outdoor targets at a distance of 270 m. The intensity of the transmitted waveform was repeatedly modulated by a unipolar representation of a 4003 bits-long Legendre sequence, with a symbol duration of 1 ns (ranging resolution of 15 cm). The range-finder beam was in partial overlap with two white paper targets, separated in depth by 1.2 m. The trace was acquired at an SNR of −29 dB over 3.1 ms.

Compared with potential implementations based on analog noise, such as the output of an optical amplifier, the carefully constructed modulation sequence provides superior correlation properties. The correlation sidelobes of the sequence are perfectly zero, whereas those of amplifier noise are not. This advantage becomes significant in measurements taken at high SNRs, in which sequence coding would provide better recognition of multiple, weak targets. Since simple direct modulation is employed in our setup, the extra cost associated with sequence coding is marginal.

An important potential advantage of the proposed method, with respect to ToF range-finders, is its possible implementation using small-form factor, readily available low-cost components. Our experiments already make use of an SFP Ethernet transmitter. Future work would include the use of tapered semiconductor optical amplifiers instead of EDFAs, to realize integrated, miniaturized transmitters. In addition, the transmitter and receiver apertures may be combined to a single lens in a mono-static configuration, with proper separation between outgoing and incoming waveforms [17].

Appendix
Statistical Correlation Among Noise-Induced Sidelobes

Consider two sidelobes of the sampled trace at the receiver output, following cross-correlation processing, at offsets $p \neq q$, $p, q \neq 0$. Due to the perfect sidelobe properties of the cross-correlation between the transmitted unipolar sequence $\hat{L_m}$ and its Legendre reference sequence L_m, the detected signal echo S_m contributes zero sidelobes. Non-zero sidelobes emerge from the cross-correlation between the additive noise term n_m and the reference

$$sl_p = \sum_{k=0}^{N-1} n_k L_{(k+p) \bmod N}, \quad sl_q = \sum_{k=0}^{N-1} n_k L_{(k+q) \bmod N}. \tag{12}$$

The statistical correlation between the two sidelobes is defined by

$$\alpha_{pq} = \left\langle \sum_{k,l=0}^{N-1} n_k L_{(k+p) \bmod N} n_l L_{(l+q) \bmod N} \right\rangle = \sum_{k,l=0}^{N-1} L_{(k+p) \bmod N} L_{(l+q) \bmod N} \langle n_k n_l \rangle. \tag{13}$$

The additive noise samples n_m are of zero mean and statistically independent of one another. Consequently, all terms in the double sum for which $k \neq l$ vanish, since $\langle n_k n_l \rangle = \langle n_k \rangle \langle n_l \rangle = 0$. In

the remaining terms $k = l$, the expectation values $\langle n_k^2 \rangle$ equal σ_n^2 for all k. The statistical correlation between the two sidelobes thus takes the form

$$\alpha_{pq} = \sum_{k=0}^{N-1} L_{(k+p) \bmod N} L_{(k+q) \bmod N} \langle n_k^2 \rangle = \sigma_n^2 \sum_{k=0}^{N-1} L_{(k+p) \bmod N} L_{(k+q) \bmod N}. \tag{14}$$

The expression within the sum is by definition an auto-correlation sidelobe of the original, bipolar Legendre sequence. All sidelobes of these sequences equal −1. We therefore obtain

$$\alpha_{pq} = \sigma_n^2 \sum_{k=0}^{N-1} L_{(k+p) \bmod N} L_{(k+q) \bmod N} = -\sigma_n^2. \tag{15}$$

The variance of each individual, noise-induced correlation sidelobe is given by $N\sigma_n^2$. Hence, the normalized correlation coefficient between any pair of sidelobes equals

$$r \equiv \frac{|\alpha_{pq}|}{\sqrt{N\sigma_n^2 N\sigma_n^2}} = \frac{1}{N}. \tag{16}$$

While this residual statistical correlation between any pair of sidelobes is weak, it is still nonzero. Therefore, the order statistics formula of (6) does not strictly apply to the PDF of the highest sidelobe. Nevertheless, the numerical analysis reported in Section 3 and the controlled experiments of Section 5 show that the approximate PDF, which is based on the assumption of statistical independence among sidelobes, does provide a useful estimate for system performance.

Acknowledgment

The authors thank Dr. Y. Noam from the Faculty of Engineering, Bar-Ilan University, for discussions regarding order statistics of noise-induced sidelobes.

References

[1] R. D. Richmond and S. C. Cain, *Direct-Detection LADAR Systems*. Bellingham, WA, USA: SPIE, 2010.
[2] M.-C. Amann, T. Bosch, M. Lescure, R. Myllyl, and M. Rioux, "Laser ranging: A critical review of usual techniques for distance measurement," *Opt. Eng.*, vol. 40, no. 1, pp. 10–19, 2001.
[3] F. Blais, "Review of 20 years of range sensor development," *J Electron. Imaging*, vol. 13, no. 1, pp. 231–240, 2004.
[4] C. E. Cook and M. Bernfeld, *Radar Signals: An Introduction to Theory and Application*. New York, NY, USA: Academic, 1967.
[5] N. Levenon and E. Mozeson, *Radar Signals*. New York, NY, USA: Wiley, 2004.
[6] D. Mermelstein, M. Biton, S. Sternklar, and E. Granot, "Fiber-optic range sensing based on amplified spontaneous emission noise radar with Kramers-Kronig phase retrieval," in *Proc. IEEE CLEO CD*, 2011, pp. 1–2.
[7] N. Levanon, "Noncoherent pulse compression," *IEEE Trans. Aerosp. Electron. Syst.*, vol. 42, no. 2, pp. 756–765, Apr. 2006.
[8] D. Kravitz, D. Grodensky, N. Levanon, and A. Zadok, "High-resolution low-sidelobe laser ranging based on incoherent pulse compression," *IEEE Photon. Technol. Lett.*, vol. 24, no. 23, pp. 2119–2121, Dec. 2012.
[9] Y. London *et al.*, "High-resolution long-range distributed Brillouin analysis using dual-layer phase and amplitude coding," *Opt. Exp.*, vol. 22, no. 22, pp. 27144–27158, Nov. 2014.
[10] A. Ilovitsh, E. Preter, N. Levanon, and Z. Zalevsky, "Time multiplexing super resolution using a Barker-based array," *Opt. Lett.*, vol. 40, no. 2, pp. 163–165, Jan. 2015.
[11] N. Levanon, I. Cohen, N. Arbel, and A. Zadok, "Non-coherent pulse compression-aperiodic and periodic waveforms," *IET Radar Sonar Navig.*, vol. 10, no. 1, pp. 216–224, 2016.
[12] N. Arbel, L. Hirschbrand, S. Weiss, N. Levanon, and A. Zadok, "Continuous-wave laser range finder based on incoherent compression of periodic sequences," in *Proc. IEEE CLEO*, 2015, pp. 1–2.
[13] E. C. Farnett and G. H. Stevens, "Pulse compression radar," in *Radar Handbook*, 3rd ed. M. I. Skolnik, Ed. New York, NY, USA: McGraw-Hill, Ch. 8, 2008.
[14] N. Takeuchi, N. Sugimoto, H. Baba, and K. Sakurai, "Random modulation CW lidar," *Appl. Opt.*, vol. 22, no. 9, pp. 1382–1386, 1983.
[15] P. Rieger and A. Ulrich, "Resolving range ambiguities in high-repetition rate airborne light detection and ranging applications," *J. Appl. Remote Sens.*, vol. 6, no. 1, 2012, Art. ID 063552.
[16] H. O. Lancaster, *Chi-Square Distribution*. New York, NY, USA: Wiley, 1969.
[17] J. Leach, S. Chinn, and L. Goldberg, "Monostatic all-fiber rangefinder system," in *Proc. IEEE CLEO*, 2015, pp. 1–2.